

# Robust parametrically varying attitude controller designs for the X-33 vehicle

**Conference Paper****Author(s):**

Smith, Roy ; Ahmed, Asif

**Publication date:**

2000

**Permanent link:**

<https://doi.org/10.3929/ethz-b-000671602>

**Rights / license:**

[In Copyright - Non-Commercial Use Permitted](#)

**Originally published in:**

AIAA Guidance, Navigation and Control Conference and Exhibit, <https://doi.org/10.2514/6.2000-4158>

# ROBUST PARAMETRICALLY VARYING ATTITUDE CONTROLLER DESIGNS FOR THE X-33 VEHICLE

Roy Smith\*

Asif Ahmed†

## ABSTRACT

Robust linear parameter varying (LPV) control design techniques are applied to the attitude control of the X-33, a single-stage to orbit prototype vehicle. The focus of the research is to develop techniques which will allow for a variety of trajectories without significant redesign of the control system. The LPV design method is described, and applied to a representative problem: control of the pitch axis dynamics during ascent. The work is on-going and this paper details the design problem formulation.

## 1 INTRODUCTION

This paper reports on research into the design of attitude controllers for the X-33; a single-stage-to-orbit prototype vehicle. The X-33 is equipped with a novel thrust vectoring aerospike engine, as well as aerodynamic surfaces and reaction control thrusters.

The flight path typically goes from lift-off at the Earth's surface to an altitude of 54 km (180,000 feet) and back to ground level for a runway landing. Attitude control is a challenging problem because of the wide variation in the dynamic behavior along the flight path. The traditional gain scheduling approach involves selecting a large number of operating points along the flight path and designing a fixed structure linear controller for each. The final control is implemented by interpolating between the controllers at each point on the flight path. This design approach is time consuming and does not lend itself to rapid trajectory redesign.

The Marshall Space Flight Center (MSFC) is supporting a research program investigating alternative attitude control design methods for the X-33 vehicle.

\*Senior member AIAA, Dept. Electrical & Computer Engineering, University of California, Santa Barbara, CA 93106.

†Guidance and Control, MS 198-326, Jet Propulsion Laboratory, California Institute of Technology, 4800 Oak Grove Drive, Pasadena, CA 91109.

Our work under this program involves the application of the robust linear parametrically varying (LPV) methods to the attitude control problem. Such methods have been developed in recent years by several research groups. See [1, 2, 3, 4, 5] and the references therein.

The LPV design approach gives controllers which can be viewed as being continuously scheduled as a function of measured (or estimated) variables. The methodology also has the advantage of enabling the control problem (trajectory tracking and disturbance rejection) to be cast in a robust control framework, which also gives a means of analyzing robustness with respect to unmodeled dynamics. Examples of typical unmodeled dynamics in this application domain include: fuel sloshing, structural vibration modes, aerodynamic coefficients, and thrust. Section 3 gives a more detailed description of the LPV design method, and Section 4 formulates a specific design problem for the X-33 vehicle. For prior applications of this approach to flight control problems see [6, 7] and [8].

## 2 X-33 ATTITUDE CONTROL

### 2.1 Overview

The trajectory is divided into two distinct modes. The ascent mode starts at lift-off and continues to the main engine cut-off in the upper atmosphere. The transition and entry mode begins at main engine cut-off and ends just prior to the final landing approach. The current design has separate guidance and attitude controllers for each mode.

In ascent mode the aerosurfaces and the main engine thrust vectoring are the actuators for the attitude maneuvering. During the transition and entry mode the main engine is shut off and attitude maneuvering is available through the reaction control system—consisting of ten 500 pound reaction jets—and the aerosurfaces. Figure 1 illustrates the X-33 vehicle and aerosurface actuators.

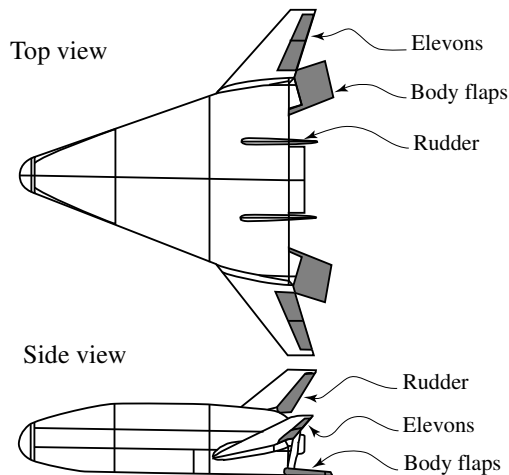


Figure 1: Illustration of the X-33 vehicle showing the aerosurface actuators

The trajectory guidance and attitude control are handled by separate modules in the flight control system. In ascent mode the guidance module generates the engine thrust commands and a reference attitude, which is passed to the attitude controller in the form of an inertial to body quaternion and reference roll, pitch, and yaw rates. The body axis rate commands can be used to implement velocity or derivative feedback.

A navigation module provides estimates of the inertial to body quaternion, as well as estimates of the roll, pitch, and yaw rates. Estimates of the angle-of-attack,  $\alpha$ , and the side-slip angle,  $\beta$ , are also available. For portions of the flight, an air-data system provides measurements of these quantities.

## 2.2 LPV Application Issues

In common with the existing design methodology, the LPV approach leads to a gain scheduled controller. However the scheduling parameters are based on environmental, vehicle, and guidance variables, rather than the flight path. This means that the LPV design will be applicable to an envelope of flight conditions rather than a particular trajectory. Redesign is not required for trajectories that remain in the parameter design envelope.

The LPV controller is calculated as an algebraic function of the measured/estimated scheduling variables. This contrasts with the standard approach of using table lookups for scheduled gains and provides a reduction in the memory requirements. Computa-

tional requirements are similar to existing methodologies.

It is important to note that the LPV methodology requires a (possibly nonlinear) differential equation based model. The system dynamics are not difficult to handle in this context; a more challenging problem arises with the aerodynamic coefficients. Wind tunnel testing and CFD code are used to produce lookup table based coefficients, typically as a function of  $\alpha$ ,  $\beta$ , Mach number, and in the case of aeroactuator surfaces, deflection angle. To apply the LPV methodology the coefficients must be modeled as nonlinear functions of these parameters. This involves the application of multi-dimensional curve fitting, and gives a trade-off between model fidelity and model complexity.

The parametric approximation of the aerodynamic database represents a significant investment in time. However the approximation is explicit and the approximation errors can be quantified and their effects analyzed via the robust control analysis.

## 2.3 Design problem

A representative problem was chosen to illustrate the application of LPV techniques. This was selected to be pitch axis control during ascent for velocities greater than Mach 2. The existing ascent controller has independent pitch axis and lateral axis control, which means that the LPV design can be integrated into the existing controller for testing. The velocity range begins at approximately 125 seconds after take-off. There is less aerodynamic coefficient variation for velocities above Mach 2 which simplifies the aerodynamic parameter fitting aspects of the problem. Section 4 describes the problem in detail.

The restricted pitch axis problem is still representative of the difficulties that will be encountered in an LPV design for the complete attitude controller. The issues addressed here include: parametric modeling on the aerodynamic coefficients; wide variation in effective actuator gain due to the variation in dynamic pressure; and significant center-of-mass and inertia variation over the operating range.

## 3 LPV DESIGN METHODOLOGY

The discussion given here follows the approach presented by Helmersson [5]. Figure 2 illustrates the manner in which the design problem is formulated.

The system,  $\tilde{G}(\tilde{\Theta})$ , is a parametrically dependent

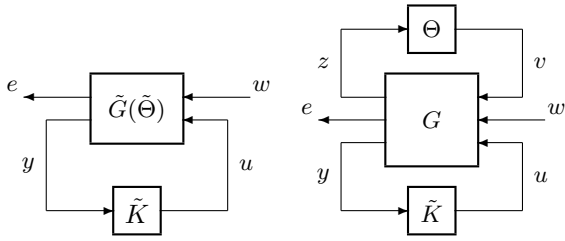


Figure 2: Block diagram illustration of the equivalent non-linear model frameworks.  $\tilde{G}(\tilde{\Theta})$  is a nonlinear input-output representation and  $G$  is an LTI system.

interconnection, with parameter vector  $\tilde{\Theta}$ , specifying the design problem. The input vector,  $w$ , represents unknown, bounded inputs; in our case, guidance commands, sensor noise, thrust and environmental disturbances. The error signals,  $e$ , are those quantities which are required to be small, in a weighted sense: tracking errors, attitude deviations and actuation effort. The formal specification of the controller performance requirement is that the norm of closed-loop transfer function from  $w$  to  $e$  (denoted by  $\mathcal{F}_l(\tilde{G}(\tilde{\Theta}), \tilde{K})$ , where  $l$  indicates that the lower loop is closed) is small,

$$\sup_{\|w\|_2 \leq 1} \|e\|_2 = \|\mathcal{F}_l(\tilde{G}(\tilde{\Theta}), \tilde{K})\|_\infty < 1.$$

Weighting functions can specify frequency domain performance requirements and are included within  $\tilde{G}(\tilde{\Theta})$ .

The system is a nonlinear function of a parameter vector,  $\tilde{\Theta}$ . We can also include in  $\tilde{\Theta}$  unknown bounded parameters (or perturbations) which represent modeling uncertainty.

Known or estimated parameters—for example Mach number, angle-of-attack, and dynamic pressure—are denoted by  $\eta_i, i = 1, \dots, r$ . This notation assumes  $r$  such parameters. Each parameter,  $\eta_i$ , may appear repeatedly in the representation and the values  $n_i, i = 1, \dots, r$ , denote the respective number of occurrences of  $\eta_i$  in  $\tilde{\Theta}$ . The repetition of parameters allows for the modeling of polynomial dependence of the parameters. For example, if  $\eta_1 = V$ , and  $V^2$  appears in the nonlinear model, then we would require  $n_1 \geq 2$ . In practice we normalize the parameters so  $|\eta_i| \leq 1$  in the range of desired operation.

Unknown, but bounded perturbations may also appear in  $\tilde{\Theta}$  and are denoted by  $\delta_j, j = 1, \dots, s$ . The  $\delta_j$  may also appear repeatedly, and we denote the

number of repetitions of  $\delta_j$  by  $m_j$ . The unknown perturbations are typically used to model the effects of dynamic uncertainty. Examples include the effects of unmodeled slosh or flex modes. The model is again normalized so that  $|\delta_j| \leq 1$ . Determining this normalization amounts to estimating the level of uncertainty we have about the unmodeled dynamics.

There is a clear distinction between  $\eta_i$  and  $\delta_j$ . Under operation, the controller will have access to a measurement of  $\eta_i$  and these will in effect be the scheduling variables. In contrast the  $\delta_j$  are unknown; the controller must be able to operate satisfactorily for all possible  $\delta_j$  with  $|\delta_j| \leq 1$ .

The nonlinear model,  $\tilde{G}(\tilde{\Theta})$ , is reformulated as the linear fractional transformation (LFT) illustrated in the right hand diagram of Figure 2. The notation used to separate  $\Theta$  into an upper closed-loop block is,  $\tilde{G}(\tilde{\Theta}) = \mathcal{F}_u(G, \Theta)$ . In this case,  $G$  is now a linear time invariant (LTI) system, and  $\Theta$  is a block diagonal matrix of parameters,

$$\Theta = \text{diag}(\eta_1 I_{n_1}, \dots, \eta_r I_{n_r}, \delta_1 I_{m_1}, \dots, \delta_s I_{m_s}).$$

The design objective is to find a controller,  $\tilde{K}$ , using measurements,  $y$ , and actuators,  $u$ , to ensure that  $\mathcal{F}_l(\mathcal{F}_u(G, \Theta), \tilde{K})$  is stable and  $\|\mathcal{F}_l(\mathcal{F}_u(G, \Theta), \tilde{K})\|_\infty < 1$  for all  $\Theta$ ,  $\|\Theta\| \leq 1$ . In the standard robust control framework,  $\tilde{K}$  is a single LTI controller. In the LPV framework we allow  $\tilde{K}$  to depend on the known (or estimated) parameters  $\eta_1, \dots, \eta_r$ . The controller dependence on  $\eta$ , is again in the LFT framework,

$$\tilde{K} = \mathcal{F}_l(K, \eta_K),$$

where  $K$  is now an LTI system. The notation  $\eta_K$  reflects the fact that the controller maintains an estimate of the system parameters,  $\eta$  (or  $\eta_G$  in the subsequent discussion). The complete interconnection is illustrated in Figure 3. The controller,  $\mathcal{F}_l(K, \eta_K)$ , can be interpreted as a continuously gain scheduled controller where  $\eta_K$  (which are estimates of  $\eta_G$ ) are the scheduling parameters.

This representation has the advantage that both  $G$  and  $K$  are LTI systems with state-space representations, allowing the design problem to be formulated in terms of the state-space matrices of  $G$ . The parameters,  $\eta_G$ ,  $\eta_K$ , and the perturbations,  $\delta$ , can be represented as either real or complex valued.

To simplify the discussion, we will initially assume that there are no perturbations,  $\delta$ . The state-space representation for  $G$ , with state vector  $x_G$ , can be

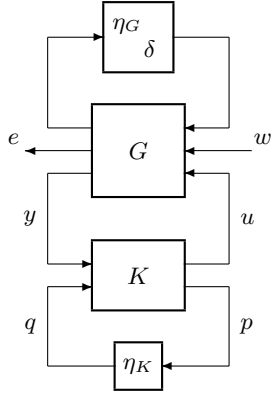


Figure 3: Closed-loop LPV design framework with LFT representations of the plant,  $\mathcal{F}_u(G, (\eta_G, \delta))$ , and the controller,  $\mathcal{F}_l(K, \eta_K)$

written as,

$$\begin{bmatrix} x_G(k+1) \\ z(k) \\ e(k) \\ y(k) \end{bmatrix} = \left[ \begin{array}{c|c} A & B \\ \hline C & D \end{array} \right] \begin{bmatrix} x_G(k) \\ v(k) \\ w(k) \\ u(k) \end{bmatrix}.$$

with  $B = [B_1, B_2, B_3]$ ,  $C = [C_1, C_2, C_3]^T$ , and

$$D = \begin{bmatrix} D_{11} & D_{12} & D_{13} \\ D_{21} & D_{22} & D_{23} \\ D_{31} & D_{32} & 0 \end{bmatrix}.$$

The zero term for  $D_{33}$  is without loss of generality and can be removed via a loop shifting operation. The model,  $\mathcal{F}_u(G, \Theta)$ , is completely specified by the additional equations which effectively close the upper loop, giving a discrete-time input-output transfer function.

$$\begin{aligned} x_G(k) &= z^{-1}x_G(k+1) \\ v(k) &= \eta_G z(k). \end{aligned}$$

To proceed augment the state-space interconnection to create inputs and outputs (including the state equations) for the controller. Define the matrices,  $Q$ ,

$U$ , and  $V$ , by

$$\left[ \begin{array}{c} x_G(k+1) \\ x_K(k+1) \\ z(k) \\ p(k) \\ e(k) \\ \hline x_K(k) \\ y(k) \\ q(k) \end{array} \right] = \left[ \begin{array}{c|c} Q & U \\ \hline V & 0 \end{array} \right] \left[ \begin{array}{c} x_G(k) \\ x_K(k) \\ v(k) \\ q(k) \\ w(k) \\ \hline x_K(k+1) \\ u(k) \\ p(k) \end{array} \right],$$

where

$$Q = \begin{bmatrix} A & 0 & B_1 & 0 & B_2 \\ 0 & 0 & 0 & 0 & 0 \\ C_1 & 0 & D_{11} & 0 & D_{12} \\ 0 & 0 & 0 & 0 & 0 \\ C_2 & 0 & D_{21} & 0 & D_{22} \end{bmatrix},$$

$$U = \begin{bmatrix} 0 & B_3 & 0 \\ I & 0 & 0 \\ 0 & D_{13} & 0 \\ 0 & 0 & I \\ 0 & D_{23} & 0 \end{bmatrix},$$

and

$$V = \begin{bmatrix} 0 & I & 0 & 0 & 0 \\ C_3 & 0 & D_{31} & 0 & D_{32} \\ 0 & 0 & 0 & I & 0 \end{bmatrix}.$$

Now the problem can be formulated as the search for a constant matrix,  $\bar{K}$  with the closed-loop given by,

$$\left[ \begin{array}{c} x_G(k+1) \\ x_K(k+1) \\ z(k) \\ p(k) \\ e(k) \end{array} \right] = [Q + U\bar{K}V^*] \left[ \begin{array}{c} x_G(k) \\ x_K(k) \\ v(k) \\ q(k) \\ w(k) \end{array} \right],$$

and

$$\begin{aligned} x_G(k) &= z^{-1}x_G(k+1), \\ x_K(k) &= z^{-1}x_K(k+1), \\ v(k) &= \eta_G z(k) \\ q(k) &= \eta_K p(k) \end{aligned}$$

The controller equations are also evident from the partitioning,

$$\left[ \begin{array}{c} x_K(k+1) \\ u(k) \\ p(k) \end{array} \right] = \bar{K} \left[ \begin{array}{c} x_K(k) \\ y(k) \\ q(k) \end{array} \right],$$

$$x_K(k) = z^{-1}x_K(k+1), \quad \text{and} \quad q(k) = \eta_K p(k).$$

In the controller implementation,  $\eta_K$  is measured, or estimated, from the environmental parameters. Ideally  $\eta_K = \eta_G$ , although it is possible to model mismatch in the parameter estimates by the inclusion of an additional  $\delta_j$  term.

The existence of a  $\bar{K}$  giving a stable closed-loop system, and satisfying

$$\|\mathcal{F}_l(\mathcal{F}_u(G, \eta_G), \mathcal{F}_l(K, \eta_K))\|_\infty \leq 1$$

for all  $|\eta_G| = |\eta_K| \leq 1$ , is equivalent to the existence of positive definite matrices,

$$R = \text{diag}(R_x, R_\eta, I),$$

and

$$S = \text{diag}(S_x, S_\eta, I),$$

such that

$$\begin{bmatrix} S_x & I \\ I & R_x \end{bmatrix} \geq 0, \quad \begin{bmatrix} S_\eta & I \\ I & R_\eta \end{bmatrix} \geq 0,$$

$$\begin{bmatrix} V^\perp & 0 \\ 0 & I \end{bmatrix} \begin{bmatrix} \Gamma_S Q - Q^* \Gamma_S - P_S & Q^* P_S \\ P_S Q & -P_S \end{bmatrix} \begin{bmatrix} V^\perp & 0 \\ 0 & I \end{bmatrix}^* < 0,$$

$$\begin{bmatrix} U^\perp & 0 \\ 0 & I \end{bmatrix} \begin{bmatrix} \Gamma_R Q^* - Q \Gamma_R - P_R & Q P_R \\ P_R Q^* & -P_R \end{bmatrix} \begin{bmatrix} U^\perp & 0 \\ 0 & I \end{bmatrix}^* < 0,$$

where we have expressed  $S$  and  $R$  as,

$$S = P_S + \Gamma_S, \quad P_S^* = P_S > 0, \quad \Gamma_S^* = -\Gamma_S,$$

and

$$R = P_R + \Gamma_R, \quad P_R^* = P_R > 0, \quad \Gamma_R^* = -\Gamma_R.$$

In the problem formulated here, we have implicitly chosen  $\dim(x_K) = \dim(x_G)$  which gives linear matrix inequality (LMI) expressions for the existence of  $\bar{K}$ , leading to a convex optimization problem.

If we include unmodeled dynamics ( $s \neq 0$ ) then we must further partition the identity matrices included in the definition of  $S$  and  $R$ , and include rank constraints on these matrices. The rank constraints are not convex, which significantly complicates the search for a solution. This situation is analogous to that occurring in the robust control design problem with structured uncertainty and it can be handled in a similar manner. A convex upper bound problem is formulated by applying scaling matrices on the system inputs and outputs. An iterative procedure, consisting of a controller design for the rescaled system, and a recalculation of the scaling matrices, is used to search for a matrix  $\bar{K}$  meeting the above conditions. This iteration is equivalent to the  $D$ - $K$  iteration applied in the linear robust control case.

## 4 PITCH AXIS CONTROL PROBLEM FORMULATION

### 4.1 Nonlinear pitch axis model

An LPV model of the vehicle longitudinal axis dynamics is developed and used to create a control design interconnection ( $\mathcal{F}_u(G, \eta)$  in the above). For simplicity, we initially assume that the side-slip angle,  $\beta$ , is zero. Three actuators are available for pitch axis control:  $u_{eng}$  (engine thrust in  $z$ -body direction);  $u_{bf}$  (body flaps); and  $u_{el}$  (elevons). The model equation development follows that in Etkin [9]. The particular formulation of the aerodynamic effects is based on that provided in the MSFC simulation.

The simplified pitch dynamics are expressed differentially for  $\alpha$  and  $q$ , the pitch rate, as follows,

$$\begin{aligned} \dot{\alpha} &= q + \frac{F_{zW}}{mV} + \frac{g}{V} \cos \Theta_W \cos \Phi_W, \\ \dot{q} &= \frac{\tau_y}{I_{yy}} + d_1, \end{aligned}$$

where  $F_{zW}$  is the force in the wind frame  $z$ -direction,  $\Theta_W$  and  $\Phi_W$  are the wind frame elevation and bank angles respectively. The higher order inertial terms are included in  $d_1$  as,

$$\begin{aligned} d_1 &= I_{zx}(r^2 - p^2) + I_{xy}(\dot{p} + qr) \\ &\quad + I_{yz}(\dot{r} - pq) + (I_{zz} - I_{xx})rp. \end{aligned}$$

As these are small and can be estimated they will be treated as a measured disturbance. We can also replace the gravity term in the  $\dot{\alpha}$  equation in the same manner:

$$d_2 = \frac{g}{V} \cos \Theta_w \cos \Phi_W.$$

The X-33 aerodynamic model is expressed in body frame coordinates, and the pitch axis  $z$  direction forces are given by,

$$F_{zB} = F_{aero zB} - \frac{QS_c}{2V} C_{nq}(\alpha, M) q + u_{eng},$$

where  $S$  is the aerodynamic reference area,  $c$  is the reference length, and  $Q = \rho V^2/2$  is the dynamic pressure. Note that the engine thrust vectoring input,  $u_{eng}$ , is simply  $T_{zB}$ , the engine thrust in the  $z$ -body direction. The  $z$ -body aerodynamic force is given by,

$$\begin{aligned} F_{aero zB} &= -QS(C_L(\alpha, M) + C_{Lbf}(\alpha, M, u_{bf}) \\ &\quad + C_{LeI}(\alpha, M, u_{el})), \end{aligned}$$

Note that the aerodynamic coefficients are functions of  $\alpha$  and Mach number,  $M$ .

The  $x$ -body force is given by a similar equation,

$$F_{xB} = F_{aero_{xB}} + T_{xB},$$

where  $T_{xB}$  is the engine thrust in the  $x$ -body direction, and the  $x$ -body aerodynamic force is given by,

$$F_{aero_{xB}} = -QS(C_D(\alpha, M) + C_{D_{bf}}(\alpha, M, u_{bf}) + C_{D_{el}}(\alpha, M, u_{el})).$$

The relationship between the body frame forces and the  $F_{zW}$  force is,

$$F_{zW} = \cos \alpha F_{zB} - \sin \alpha F_{xB}.$$

The pitch torque,  $\tau_y$ , is given by,

$$\begin{aligned} \tau_y = & QS(c(C_{pm}(\alpha, M) + C_{pmbf}(\alpha, M, u_{bf}) \\ & + C_{pmel}(\alpha, M, u_{el})) + \frac{QSc^2}{2V}C_{pmq}(\alpha, M)q \\ & + x_{eng}(m)u_{eng} + z_{eng}T_{xB} \\ & - R_x(m)F_{aero_{zB}} + R_zF_{aero_{xB}}. \end{aligned}$$

The engine force moment arms are  $x_{eng}$  and  $z_{eng}$ . Note that  $x_{eng}$  moves as fuel is expended and so is expressed here as a function of mass,  $m$ .  $R_x$  and  $R_z$  are the moment arms between the center-of-mass and center-of-pressure. Again,  $R_x$  varies with mass, and over the flight regime we are considering, changes sign.

#### 4.2 LFT model approximation

To apply the LPV approach, we must first approximate the above equations, including the aerodynamic coefficient look-up tables,  $C_L(\alpha, M)$ , etc., by linear fractional models on the scheduling parameters. This is a time consuming procedure, however it does not need to be repeated unless an aerodynamic surface is modified. Figure 4 shows an example of this approximation procedure. For simplicity we show only a representative actuation coefficient,  $C(\alpha, u)$ , assumed to be independent of  $M$ , for  $M > 2$ . Two approximations are shown to illustrate the trade-off between complexity and fidelity. The first, shown in Figure 4b), is

$$C(\alpha, u) \approx (c_1 + c_2\alpha)u,$$

and can be expressed as an LFT on  $\alpha$ . The second—simpler—approximation, shown in Figure 4c) is linear in  $u$ ;

$$C(\alpha, u) \approx c_3 u.$$

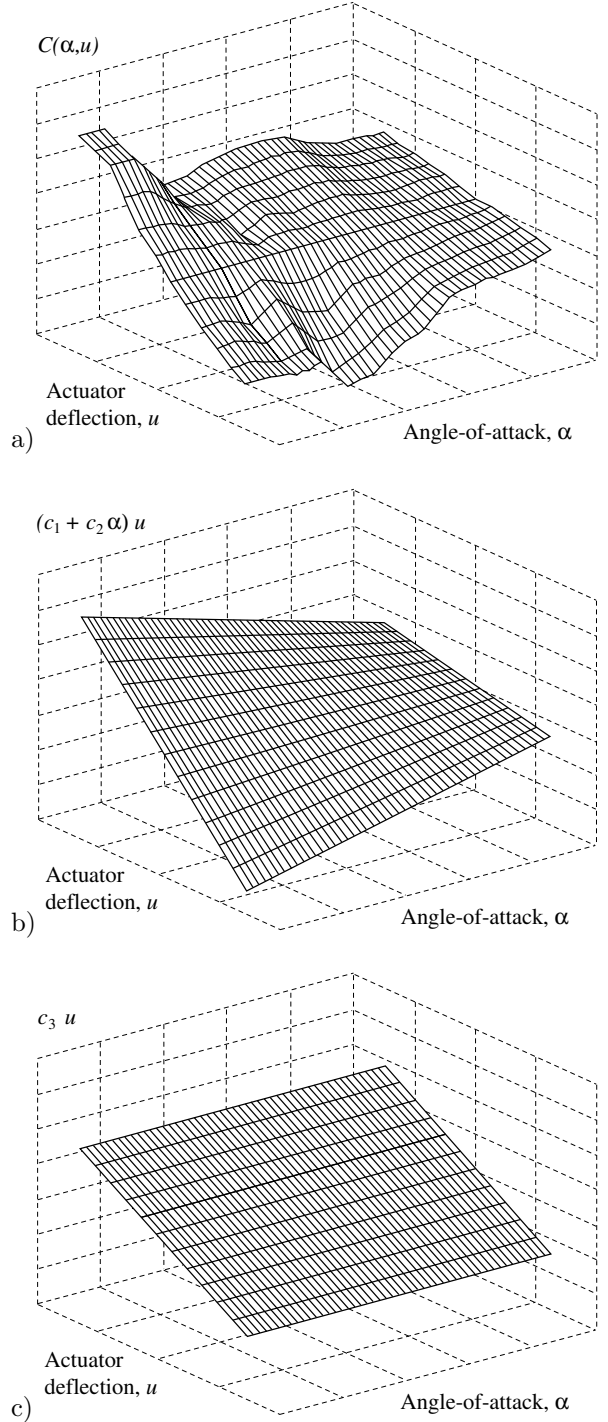


Figure 4: Aeroactuator coefficient approximation: a)  $C(\alpha, u)$  look-up table values; b) LFT approximation; c) linear approximation

The scheduling parameters are  $m$ ,  $V$ ,  $\rho$ , and  $\alpha$ . Note that as  $\alpha$  is also a state variable we must check closed-loop stability of the nonlinear interconnection after performing the design. In each case we normalize the parameters to fit in the LPV framework. For example, we replace each occurrence of  $V$  by an LFT on  $\eta_V$ ;

$$\begin{aligned} V &= \frac{(V_{\max} + V_{\min})}{2} + \frac{(V_{\max} - V_{\min})}{2} \eta_V, \\ &= \mathcal{F}_u(V_{\text{ft}}, \eta_V), \quad -1 \leq \eta_V \leq 1, \end{aligned}$$

where

$$V_{\text{ft}} = \begin{bmatrix} 0 & \frac{(V_{\max} - V_{\min})}{2} \\ 1 & \frac{(V_{\max} + V_{\min})}{2} \end{bmatrix},$$

and where  $V$  ranges between  $V_{\min}$  and  $V_{\max}$  under the specified operating conditions. Note that  $1/V$  occurs in the model and it too can be expressed in LFT form,

$$\frac{1}{V} = \mathcal{F}_u(iV_{\text{ft}}, \eta_V), \quad -1 \leq \eta_V \leq 1,$$

with

$$iV_{\text{ft}} = \begin{bmatrix} \frac{-(V_{\max} - V_{\min})}{(V_{\max} + V_{\min})} & \frac{-(V_{\max} - V_{\min})}{(V_{\max} + V_{\min})} \\ \frac{2}{(V_{\max} + V_{\min})} & \frac{-2}{(V_{\max} + V_{\min})} \end{bmatrix}.$$

This approach was applied to the nonlinear effects of  $\rho$ ,  $V$ , and  $m$ . The aerodynamic coefficients were approximated by LFTs based on  $\alpha$ . The variation of  $I_{yy}$ ,  $x_{eng}$ , and  $R_x$  was approximated by LFTs based on  $m$ . Many of the approximations are based on the fact that  $\alpha$  is typically close to zero during this flight regime.

The resulting LFT model has the form,

$$\begin{aligned} F_{zW} &= -QS(C_L + C_{L\alpha}\alpha + C_{Lbf}u_{bf} \\ &\quad + C_{Le\ell}u_{e\ell}), \\ \dot{\alpha} &= \left(1 + \frac{\rho}{4m} C_{nq}\right) q + \frac{1}{mV} F_{zW} + d_2, \\ \dot{q} &= \frac{1}{I_{yy}} \left[ \frac{QSc^2}{2V} C_{pmq} q - R_x F_{zW} \right. \\ &\quad \left. + QSc(C_{pm} + C_{pm\ell}u_{e\ell} + C_{pmbf}u_{bf}) \right. \\ &\quad \left. + x_{eng} u_{eng} + d_3 \right] + d_1. \end{aligned}$$

The torque bias due to the  $x$ -body direction thrust is modeled as a measured disturbance,

$$d_3 = z_{eng} T_{xB}.$$

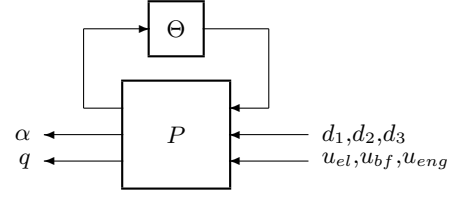


Figure 5: LFT model of the pitch axis dynamics

LFT approximations are used to model the terms,  $Q = \rho V^2/2$ ,  $1/m$ ,  $1/I_{yy}$ ,  $1/V$ ,  $\rho$ ,  $R_x$ ,  $C_{pmq}$ , and  $C_{pm\ell}$ . The resulting model is illustrated in Figure 5. The parameter block,  $\Theta$ , has the structure,

$$\Theta = \text{diag}(\eta_\alpha I_2, \eta_m I_4, \eta_V I_4, \eta_\rho I_2).$$

Note that  $P$  is linear, time-invariant, and expressed in state-space form.

#### 4.3 Design interconnection model

The LPV control design problem has been formulated for limited operating conditions (pitch axis control for  $M > 2$ ), and must be integrated into the existing controller for testing and verification. This places several constraints on the controller configuration, illustrated in Figure 6.

The upper two vector inputs in Figure 6 are the estimated values required to reconstruct the nonlinear disturbance terms,  $d_1$ ,  $d_2$ , and  $d_3$ . The next set of inputs are the scheduling parameters. The reference command inputs are specified by a pitch rate reference,  $q_{ref}$ , and a reference inertial to body quaternion,  $Q_{IBref}$ . The measurement variables are  $q$  and  $Q_{IB}$ , the estimated inertial to body quaternion. Under some flight conditions a measurement of  $\alpha$  is available from an air-data system.

The pitch axis controller is divided into several parts, and the controller structure is illustrated in Figure 7. The  $C_{pe}$  block uses a small angle approximation to derive a pitch angle error from  $Q_{IBref}$  and  $Q_{IB}$ . Driving this error to zero is a primary design objective. The pitch angle error is passed to the  $C_p$  block, along with the guidance system generated pitch rate reference,  $q_{ref}$ , and the actual pitch rate,  $q$ . The  $C_p$  block combines these objectives and generates a modified pitch rate reference,  $\tilde{q}_{ref}$ . The  $C_p$  control block has the effect of adding integral control with respect to pitch angle and is relatively simple. It is not detailed further here.



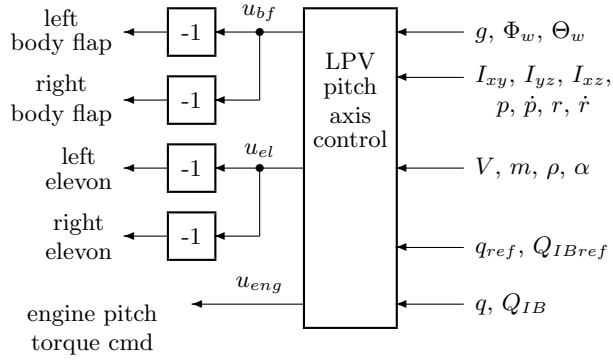


Figure 6: Controller configuration. The negative gains reflect the downward positive direction definition of the aeroactuator deflections

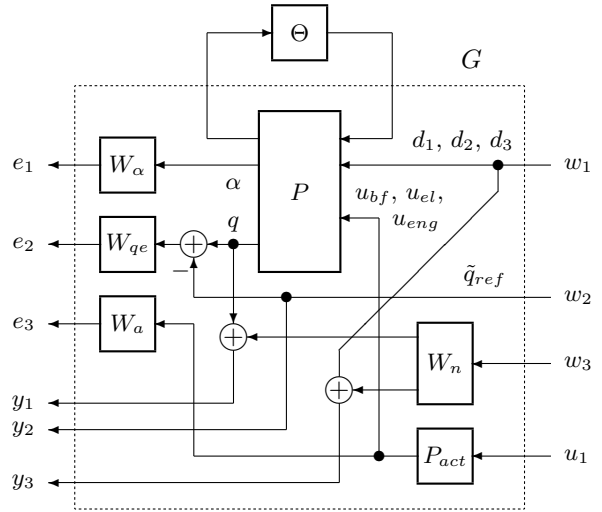


Figure 8: LPV design interconnection

The pitch rate tracking controller,  $C_q$ , is required to handle the nonlinear pitch axis dynamics and is designed via LPV methods. The remainder of the discussion focuses on  $C_q$ .

Figure 8 illustrates the LPV design interconnection for the design of the controller  $C_q$ . The input and output labels match the signals illustrated in Figure 2.

The error signals are weighted angle-of-attack (specified via  $W_\alpha$ ), weighted pitch rate error (specified via  $W_q$ ), and weighted actuation (specified via  $W_a$ ). The disturbance inputs,  $w$ , correspond to the nonlinear disturbance terms  $d_1, d_2, d_3$ ; the pitch rate reference,  $\tilde{q}_{ref}$ , and a vector valued noise signal (weighted via  $W_n$ ). The direct inclusion of a weighted angle-of-attack component in the error output is applicable only if the desired angle-of-attack is close to zero. This is the case for X-33 ascent control. For descent control the angle-of-attack is significant and the controller performance should be specified with respect to a reference  $\alpha$ .

The controller measurements,  $y$ , are pitch rate,  $q$ , plus noise, nonlinear disturbances,  $w_1$ , plus noise, and the pitch rate reference,  $\tilde{q}_{ref}$ . The controller access to  $w_1$  will effectively create a disturbance feedforward cancelation of the drift nonlinearities. The addition of bounded noise to this signal will prevent the controller from depending on an exact cancelation.

The LPV design methods outlined in Section 3 can

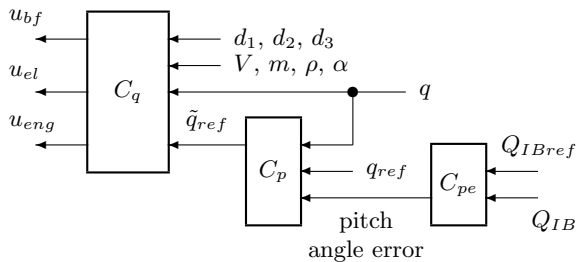


Figure 7: Multi-loop controller arrangement

be applied directly to the state-space structure,  $G$ , illustrated in Figure 8. The resulting LMI problems can be solved via optimization code provided in the MATLAB LMI toolbox.

## 5 DISCUSSION

Attitude controllers which are scheduled on the basis of the trajectory may require redesign for subsequent trajectory modifications. The LPV methods investigated here attempt to overcome this problem by basing the scheduling on environmental and vehicle parameters, effectively giving a design which is suitable for an operational envelope. The use of the robust control framework allows for the specific inclusion of a level of uncertainty in the design framework. It also provides computationally based robustness tests which allow the designer to assess the stability margins with respect to the nonlinear model. This contrasts with more standard approaches which consider the margins of linearized versions of the system along the trajectory.

A significant difficulty encountered in using the LPV approach is the formulation of the design model. The extensive lookup table based model must be reformulated in a more analytic framework; specifically LFTs on the scheduling parameters. This involves developing approximations for each of the aerodynamic coefficients. There is a trade-off between the complexity and the fidelity of these approximations. The consequences of the trade-off can only be investigated by running through the design procedure and comparing the resulting controllers' performance levels.

It is important to note that the aerodynamic approximations are explicit, and can be revisited if greater performance is required or there is a configuration change in the aerosurfaces. The explicit nature of the approximations is a significant advantage in reviewing the design prior to flight qualification.

The control problem formulated here considers only a portion of the X-33 flight conditions (ascent for  $M > 2$ ), and addresses only the pitch axis control. The problems encountered here are representative of other parts of the operating envelope, although the designs and performance trade-offs will vary.

## ACKNOWLEDGEMENTS

This research was carried out by the Jet Propulsion Laboratory, under a contract to the National Aeronautical and Space Administration. The support of

the NASA Marshall Space Flight Center is gratefully acknowledged. The authors would also like to thank the following people at MSFC for technical assistance with the Maveric and Marsyas software, as well as the model development: John Hanson, Kerry Funston, Don Krupp, Charlie Hall and Warren Adams.

## REFERENCES

- [1] G. Becker, *Quadratic Stability and Performance of Linear Parameter Varying Systems*. PhD thesis, University of California, Berkeley, 1993.
- [2] S. Shahruz and S. Behtash, "Design of controllers for linear parameter varying systems by the gain scheduling technique," *J. Mathematical Analysis and Applications*, vol. 168, pp. 195–217, 1992.
- [3] A. Packard, "Gain scheduling via linear fractional transformations," *Systems & Control Letters*, vol. 22, pp. 79–92, 1994.
- [4] G. Becker and A. Packard, "Robust performance of linear parametrically varying systems using parametrically dependent linear dynamic feedback," *Systems & Control Letters*, vol. 23, no. 3, pp. 205–215, 1994.
- [5] A. Helmersson, *Methods for Robust Gain Scheduling*. PhD thesis, Linköping University, Sweden, 1995.
- [6] P. Apkarian and J.-M. Biannic, "Self-scheduled  $H_\infty$  control of missile via linear matrix inequalities," *AIAA J. Guidance, Control & Dynamics*, vol. 18, no. 3, pp. 532–538, 1995.
- [7] F. Wu, A. Packard, and G. Balas, "LPV control design for pitch-axis missile autopilots," in *Proc. IEEE Conf. on Decision & Control*, 1995.
- [8] G. Balas, I. Fialho, A. Packard, J. Renfrow, and C. Mullaney, "On the design of LPV controllers for the F-14 aircraft lateral-directional axis during powered approach," in *Proc. American Control Conf.*, pp. 123–127, 1997.
- [9] B. Etkin, *Dynamics of Atmospheric Flight*. Wiley, 1972.